Prevention of alkali-aggregate reaction by using fiber reinforced concrete

Maria Rita P. Carvalho [(1)], Eduardo M. R. Fairbairn [(2)], Romildo D. Toledo-Filho [(3)]

(1) FTESM – Civil Engineering, Rio de Janeiro, Brazil, ritapirescarvalho@hotmail.com

(2) COPPE/UFRJ – Civil Engineering Department, Rio de Janeiro, Brazil, eduardo@coc.ufrj.br

(3) COPPE/UFRJ – Civil Engineering Department, Rio de Janeiro, Brazil, toledo@coc.ufrj.br

Abstract

This work presents an experimental program that consists in applying fiber reinforced concrete as measure to prevent structures to be affected by alkali-aggregate reaction (AAR). To prevention, steel fibers having lengths of 13 mm and 60 mm were used as reinforcement in a reactive concrete on volumetric fractions from 0.5% to 1.0. The prevention evaluation was performed by means of long-term expansion tests, microstructural techniques and cracking observation. The mechanical properties and the water absorption were also evaluated. The efficiency of using fibers to control AAR was demonstrated by this research that indicated a reduction of half the expansion in comparison with a reference concrete.

Keywords: *alkali-aggregate reaction; steel fibers experimental analysis*

1. INTRODUCTION

Several measures have been taken to prevent the expansion of the alkali-aggregate reaction in concrete. The use of a cement with a reduced content of alkalis and the use of non-reactive aggregates is the most effective way to avoid the reaction. However, as such measures are not always possible in practice, it is already proven that the use of additions of pozzolanic materials in concrete is efficient in inhibiting the expansion caused by RAA [1]. As a preventive form, studies have also shown that the incorporation of fibers in concrete restricts the expansion and, still, is able to control subsequent cracks.

There are few references concerning the influence of fibers on the development of AAR in the specialized literature. Turanli et al. [2] analysed the use of steel microfibers in fiber volume contents ranging from 1% to 7%. The authors observed that the use of fibers significantly reduced the expansion and cracking due to AAR. To proof the hypothesis of Turanli et al. [2], Garci et al. [3] developed a special type of aggregate with embedded microfibers (fiber volume of 0.5%) and observed that the expansion reduced by 25%. Ostertag et al. [4] used a mixture with fiber volume of 7% of steel microfibers and observed that the beneficial effect of steel fibers comes from the mechanical confinement of the gel produced by the reaction. Haddad and Smadi [5] evaluated the role of steel fibers (fiber volume contents of 0.5% and 1.0%) and polypropylene (0.15%). They concluded that, for these fiber volumes, the fibers contributed moderately to reduce the expansion due to AAR. However, the extent of cracking was found to be limited by the use of fibers. Park and Lee [6] analyzed the efficiency of steel fibers in mortars containing aggregates of waste glass. They observed that the addition of 1.5% of fibers to concrete containing 20% waste glass can reduce the expansion ratio up to 40% and increase the flexural strength up to 110%. Carvalho et al. [7] evaluated the influence of 6mm and 13 mm long steel microfibers in the contents of 1% and 2% in substitution of the volume of mortar in the control of the expansion generated by the RAA. The results obtained indicated a reduction of up to 61% in the expansion when 2% of 13 mm fibers were used, without compromising the main mechanical properties of the material. In the research carried out by Yazici [8], the efficiency of reactive mortars was evaluated, consisting of a cement with a high content of alkalis and basaltic aggregate, reinforced with steel fibers 6 mm long, 0.16 mm in diameter, added in the contents of 1% and 2% of the mortar volume. The results indicated that the steel fibers reduces up to 65% the expansion of the reference matrix at 14 and at the end of the test the reduction was 32% when 2% of fibers were used.

Beglarigale and Yazici [9] evaluated the effect of the alkali-silica reaction on the pull out behavior of the fibers, and it was found that the bond strength of the samples submitted to the NaOH solution at advanced ages is significantly high, which can be explained by the presence of the gel on the surface of the fibers.

The present work aims to evaluate the use of fiber to reduce the alkali-aggregate expansion. For this purpose, reactive concretes reinforced with volumetric fractions of 0.5% and 1.0% of steel fibers of 60 mm and 13 mm in length were submitted to to long-term tests. The results indicated the benefic use of fibers to limit the effects of AAR.

2. MATERIALS

2.1 Raw materials

The raw materials used for producing the concretes of the present research are detailed in a companion paper published in this conference: “Repair system of alkali-aggregate reaction by using fiber reinforced concrete” by Carvalho, M. R. P., Fairbairn, E. M. R. and Toledo-Filho, R. D.

2.2 Fibers

Two types of steel fibers (long and short) were used (see Figure 2.1). The long fiber was Dramix 80/60, with aspect ratio (l/d) of 80, 60 mm long and 0.75 mm diameter, with hooks at its ends. The short fiber was Densit/KRAMPE 65/20, with aspect ratio (l/d) of 65, 13 mm long, and 0.20 mm diameter.

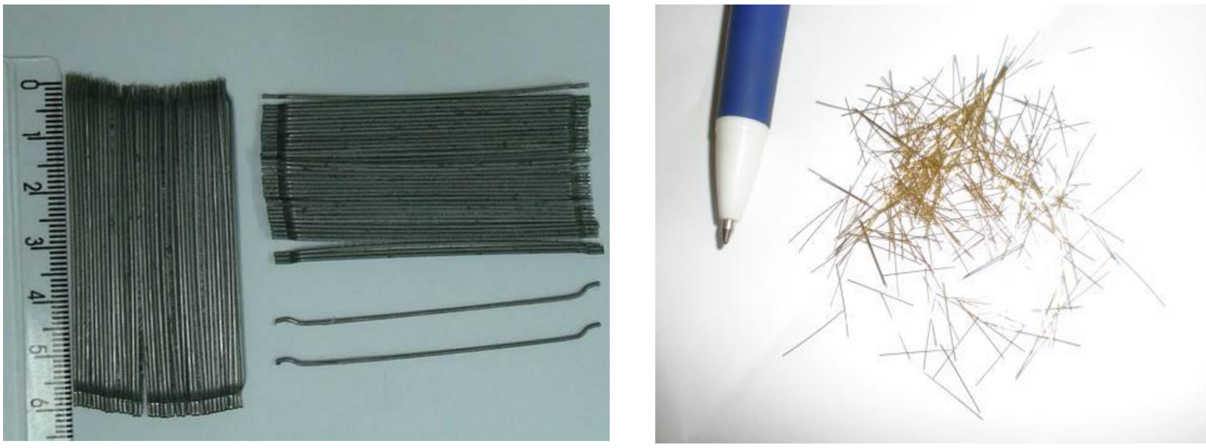

(a) Dramix 80/60 (b) Densit/KRAMPE 65/20

Figure 2.1: Types of fibers used in this research.

2.3 Reference concrete and fiber reinforced concretes

The concrete used to assess the action of fibers in the AAR had it mix-design based on the recommendations of RILEM B - TC 106-3 [10], ASTM C-1293 [11] and NBR 15577-6 [12]. However, some adjustments were made in view of the use of steel fibers in the mixture: (i) the use of superplasticizer (SP); (ii) the correction of the fines content; and (iii) the use of a viscosity modifying agent (VMA). We used a reactive coarse aggregate which is a reactive quartzite from the construction of the Furnas Hydroelectric Plant, located in the State of Minas Gerais, Brazil. Otherwise, since the cement did not have enough alkali content to provide alkali-aggregate reactivity, NaOH was added to the mixture.

The nomenclature adopted for the several materials of this research is: AB_X_Y, where AB = {RC;FC}, RC standing for Reference Concrete, and FC for Fiber Concrete; X = {0.5; 1.0} is the content of fibers (in volume) and Y = {60;13} is the fiber length in mm. The mix proportions of the concretes are displayed in Table 2.1.

Table 2.1: Mix proportions of RC

Material	Cement (kg/m3)	Sand (kg/m3)	Coarse agg. (kg/m3)	Water (kg/m3)	NaOH (kg/m3)	VMA (kg/m3)	SP (% of cement mass)
RC	433	699	1057	200	3.18	0.520	1.2
FC_0.5_60	430	696	1052	199	3.17	0.516	1.2
FC_1.0_60	428	692	1047	198	3.15	0.514	1.2
FC_0.5_13	430	696	1052	199	3.17	0.516	1.2
FC_1.0_13	428	692	1047	198	3.15	0.514	1.2

The main mechanical properties of the several concretes at 28 days are given in Table 2.2, where: f_{cc} is the compressive strength; E is the Young´s modulus; f_{cr1} is the stress at first cracking; f_{ctu} is the maximum tensile stress; Tb is the area below the load-deflection curve until deflection of 3 mm and FT is the flexural toughness factor given by JCSE-SF4 [13].

Table 2.2: Main mechanical properties at 28 days

	compression		4-point bending			
Material	f_{cc} (MPa)	E (GPa)	f_{cr1} (MPa)	f_{ctu} (MPa)	Tb (kNmm)	FT (MPa)
RC	34.3	32.2	4.7	5.6	-	-
FC_0.5_60	31.3	26.1	4.4	5.7	41.8	4.2
FC_1.0_60	38.1	30.6	5.4	8.9	76.8	7.7
FC_0.5_13	33.0	27.1	4.7	6.4	22.0	2.2
FC_1.0_13	35.4	30.3	5.0	6.2	21.7	2.2

3. EXPERIMENTAL PROGRAM

To evaluate the efficiency of fiber reinforced concrete, three cylindrical specimens of each concrete were molded in the dimensions of ϕ=147 mm x *h*=298 mm. They were cured for 28 days and then immersed in a tank containing 1N NaOH solution at a temperature of 40° C for 365 days.

In this paper, when we refer to a result corresponding to a certain time *t*, we are referring to the time of immersion of the specimen in the alkaline solution, i.e., the age of the specimen is *t* + 28 days.

The measures of the dimensional variations of the specimens were performed with the help of an equipment specially designed to measure long term volumetric deformations [14] (see Figure 3.1).

Figure 3.1: Measurement system.

4. RESULTS

4.1 Expansion

Figure 4.1a, Figure 4.1b, and Figure 4.2 illustrate the average curve of three specimens of the longitudinal ($\Delta L/L$), diametral ($\Delta D/D$) and volumetric ($\Delta V/V = \Delta L/L + 2\ \Delta D/D$) expansions, respectively, of the reference concrete (RC) compared to the fiber reinforced concretes. The dashed line in Figure 4.1a corresponds to the expansion of 0.04%, the value for which RILEM B TC 106-3 [10] and ASTM C-1293 [11] indicate the presence of reactive aggregates.

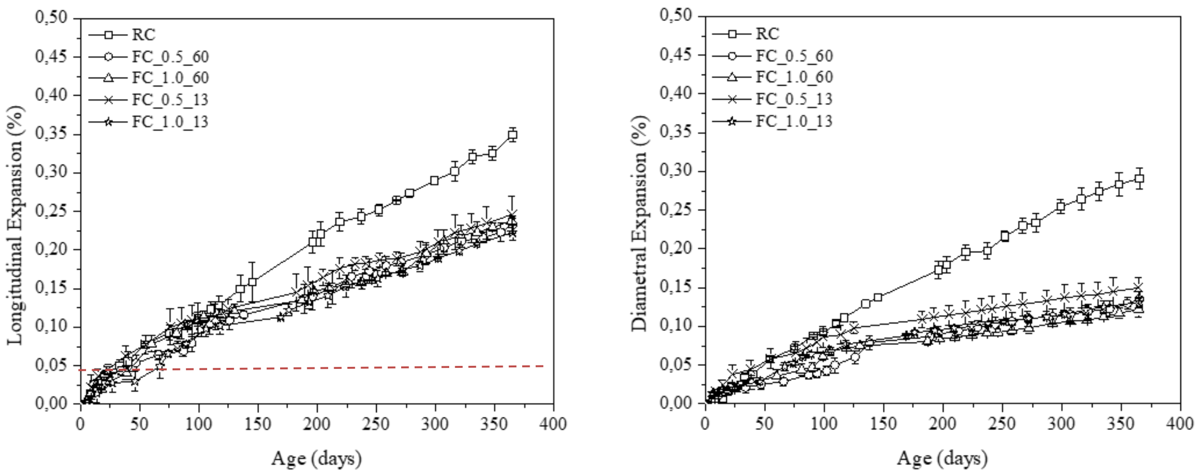

(a) (b)

Figure 4.1: Average expansion curve for RC and FC concretes (a) longitudinal (b) diametral

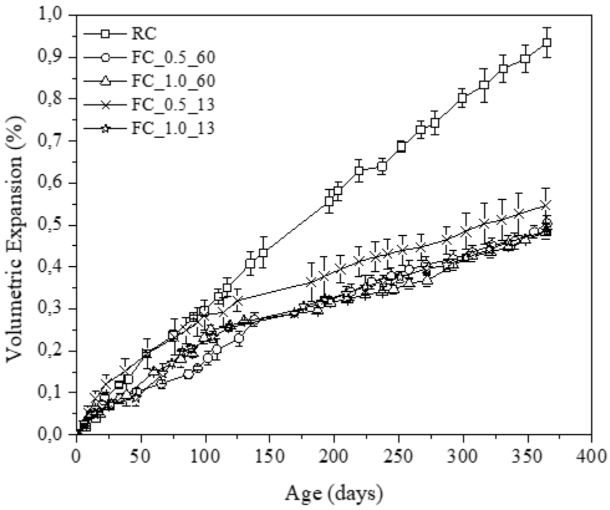

Figure 4.2: Average volumetric expansion curve for RC and FC concretes

The main measures of expansion (%) for 90, 180 and 365 days together with theirs coefficients of variation are given in Table 4.1 and Table 4.2.

Table 4.1: longitudinal and radial expansions (%) and coefficient of variation (%)

	longitudinal			Radial		
	90 days	180 days	365 days	90 days	180 days	365 days
RC	0.10 – 4.7	0.21 – 6.8	0.35 – 2.5	0.09 – 1.7	0.17 – 6.3	0.29 – 4.5
FC_0.5_60	0.08 – 13.6	0.14 – 13.9	0.23 – 4.9	0.04 – 14.2	0.10 – 11.4	0.13 – 7.6
FC_1.0_60	0.10 – 0.4	0.13 – 3.0	0.24 – 1.4	0.05 – 12.51	0.08 – 6.5	0.12 – 8.2
FC_0.5_13	0.11 – 18.4	0.15 – 16.6	0.25 – 9.7	0.08 – 15.8	0.11 – 10.2	0.15 – 8.7
FC_1.0_13	0.08 – 6.3	0.12 – 6.1	0.22 – 4.3	0.06 – 5.0	0.09 – 3.4	0.13 – 4.3

Table 4.2: volumetric expansion (%) and coefficient of variation (%)

	90 days	180 days	365 days
RC	0.28 – 1.8	0.56 – 4.9	0.93 – 3.7
FC_0.5_60	0.14 – 7.1	0.31 – 3.0	0.50 – 3.5
FC_1.0_60	0.19 – 5.9	0.30 – 2.2	0.48 – 3.5
FC_0.5_13	0.27 – 12.7	0.36 – 12.3	0.55 – 7.5
FC_1.0_13	0.21 – 4.4	0.31 – 2.2	0.49 – 0.7

For all samples, the expansion of 0.04% occurred before the age of 90 days of immersion of the specimens in the alkaline solution, that is, all mixtures showed signs of a deleterious reaction before that date.

Observing the longitudinal and radial expansions, it can be seen that for the fiber-reinforced concretes, the former is practically twice as much as the latter. This shows that if this phenomenon, already verified by Larive [15], was not considered, the conclusions of this research could have been distorted. This fact reinforces the need to use measurement equipment capable of distinguishing longitudinal and radial deformations.

The results presented above indicate, in general, that the introduction of fiber reinforcement can control the expansion caused by AAR. In the case of concrete reinforced with fibers of 60 mm in length, it was observed a reduction in the expansion in the same margin for the two fiber contents used. For concrete reinforced with 13 mm long fibers, there was an increase in mitigating the expansion of RAA with the increase in the content of fibers used.

One can notice that there is an inflection in the expansion curve of the specimens with fibers. This fact occurs after the micro-cracking of the cement matrix and the consequent action of the fibers. Although it is difficult to observe exactly the age at which cracks appear in a long-term AAR test, there are experimental evidence that the matrix showed a crack pattern at the time of inflection.

4.2 Scanning electron microscopy (SEM)

The SEM aimed to identify the presence of alkali-aggregate reaction products, in order to effectively confirm the presence of the reaction, complementing the results obtained from the long-term expansion tests. The micrographs presented the AAR products in varied morphologies corresponding to the composition of the silico-calcico-alkaline products of the reaction. The abbreviations used in the figures of the micrographs were: A - aggregate; G - RAA product; M - concrete matrix; P - pore; F - fibers; X - corresponds to the specific location of the analysis by EDS.

Figure 4.3 shows the general aspect of the matrix of a RC specimen and formation of the RAA product at 90 days inside a pore.

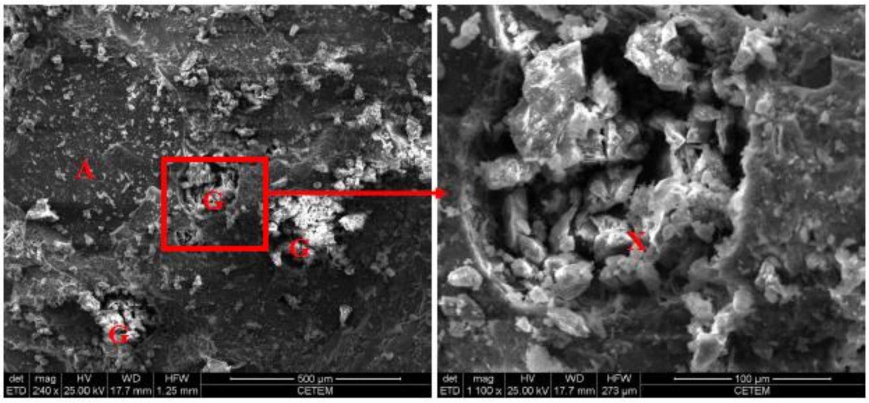

(a) (b)

Figure 4.3: RC concrete at 90 days: (a) General aspect of the concrete; (b) zoom of the pore with the presence of reaction product.

At 180 days the reaction product appeared in RC with a cracked appearance inside the pores, as well as microcracking spread in the concrete matrix (Figure 4.4).

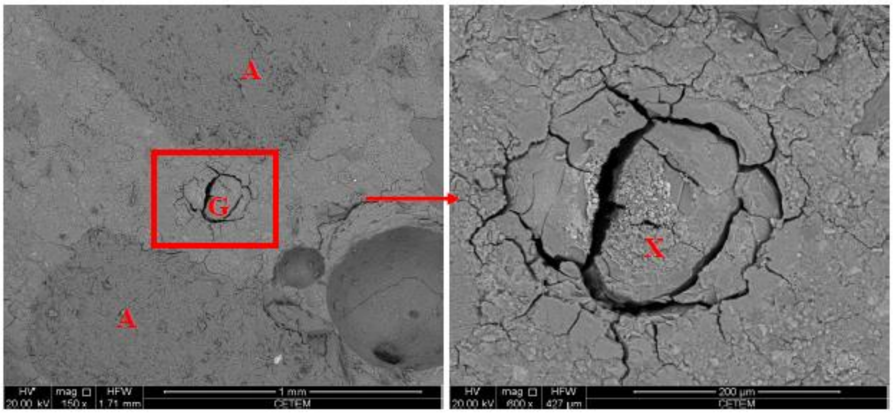

(a) (b)

Figure 4.4: RC concrete at 180 days: (a) RAA product in the microcracked matrix; (b) expansion of the reaction product.

In Figure 4.5, corresponding to the reference reactive concrete CR after 365 days, it can be observed the micro-cracked concrete matrix, presenting the products of the alkali-aggregate reaction with cracked gel and the appearance of lacy fabric.

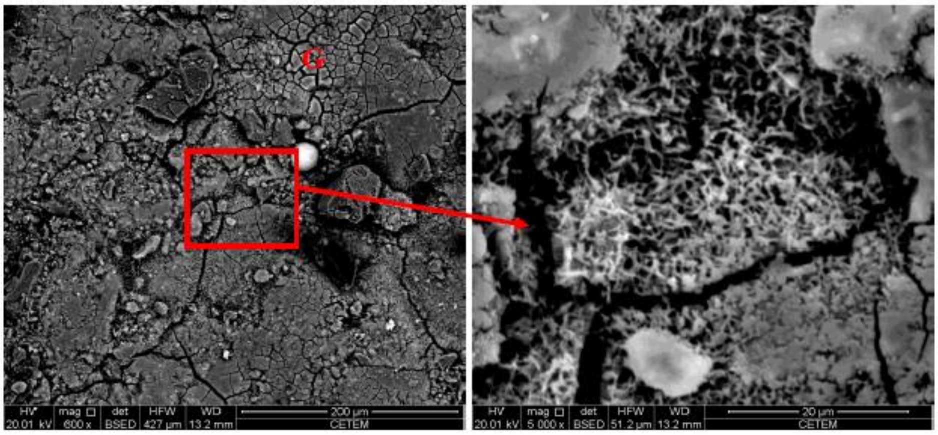

(a) (b)

Figure 4.5: RC concrete at 365 days: (a) micro-cracking of the matrix; (b) product of the reaction with a lacy appearance..

Figure 4.6 shows a micrograph of the FC_0.5_60 concrete, indicating the AAR product with cracked appearance in the vicinity of the fiber.

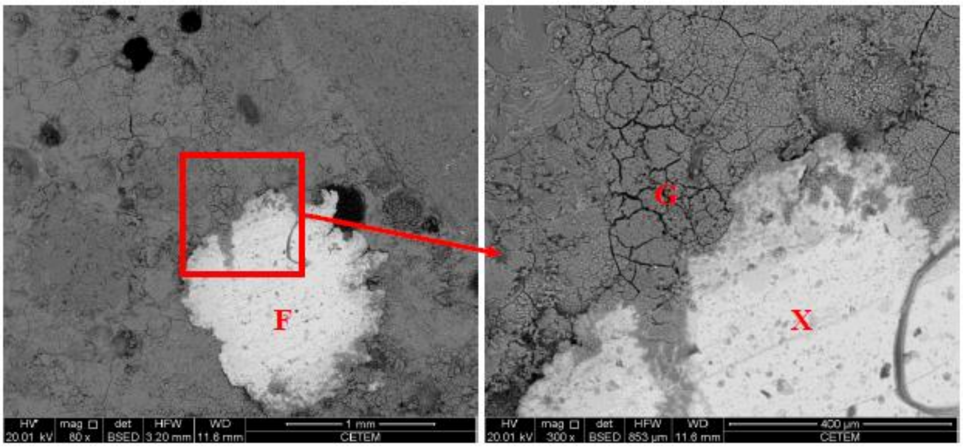

(a) (b)

Figure 4.6: FC_0.5_60 concrete at 365 days: (a) Product of the AAR reaction added in the vicinity of the steel fiber; (b) zoom of the fiber/matrix interface.

Micrographs of FC_0.5_13 and FC_1.0_13 at 365 days are shown in Figure 4.7and Figure 4.8 respectively. The. Basically, in both samples, the micro-cracked matrix was observed, with the reaction product showing a cracked appearance, located in the vicinity of the fibers, inside the pores and spread in the concrete matrix. In Figure 5.37 it was possible to observe the presence of the product of the alkali reaction aggregated on the fiber surface.

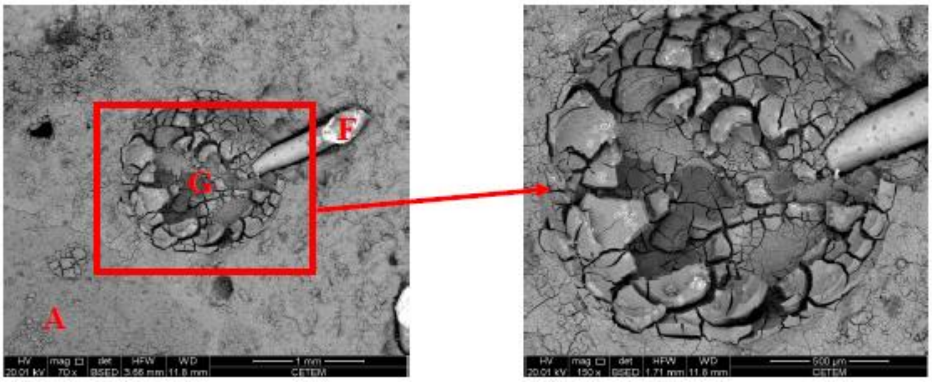

(a) (b)

Figure 4.7: FC_0.5_13 concrete at 365 days: (a) General view of concrete with fiber; (b) enlargement of the pore filled by the gel with cracked appearance.

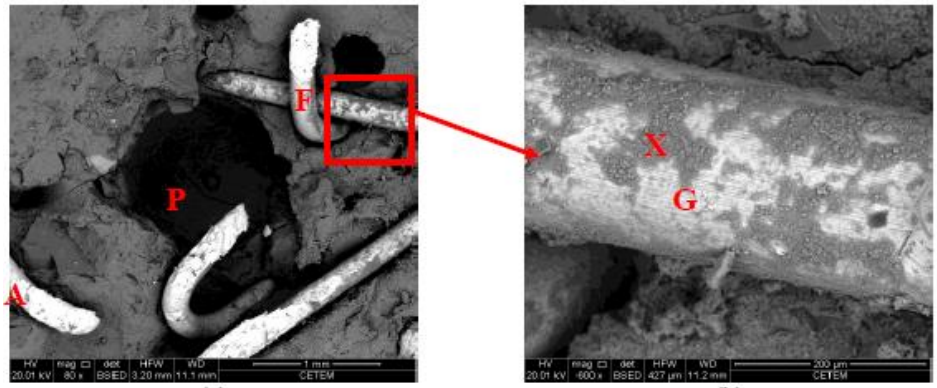

(a) (b)

Figure 4.8: FC_1,0_13 concrete at 365 days: (a) Arrangement of fibers in concrete; (b) RAA product disposed on the fiber surface.

4.3 Cracking pattern

Figure 4.9, Figure 4.10 and Figure 4.11 present typical cracking patterns for the several concretes studied in this paper. One can notice that the cracks appear mainly in the direction perpendicular to pouring direction, the same phenomenon already verified by Larive [15].

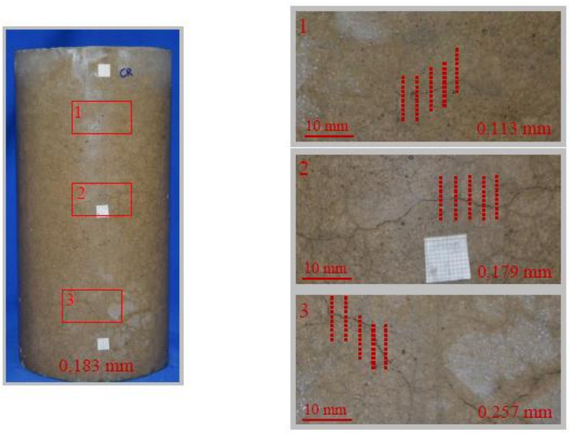

Figure 4.9: Typical cracking at 365 days for concrete RC.

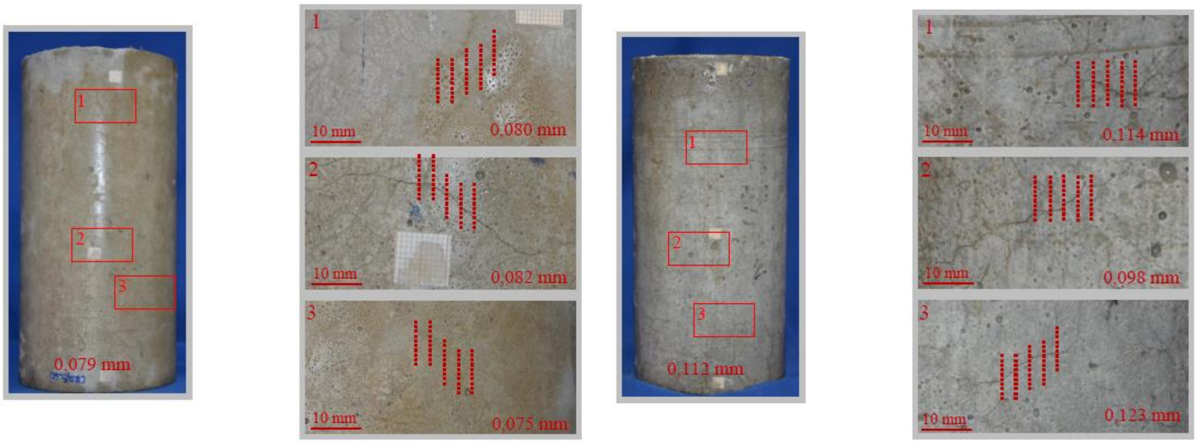

(a) (b)

Figure 4.10: Typical cracking at 365 days: (a) FC_0.5_60; (b). FC_1.0_60

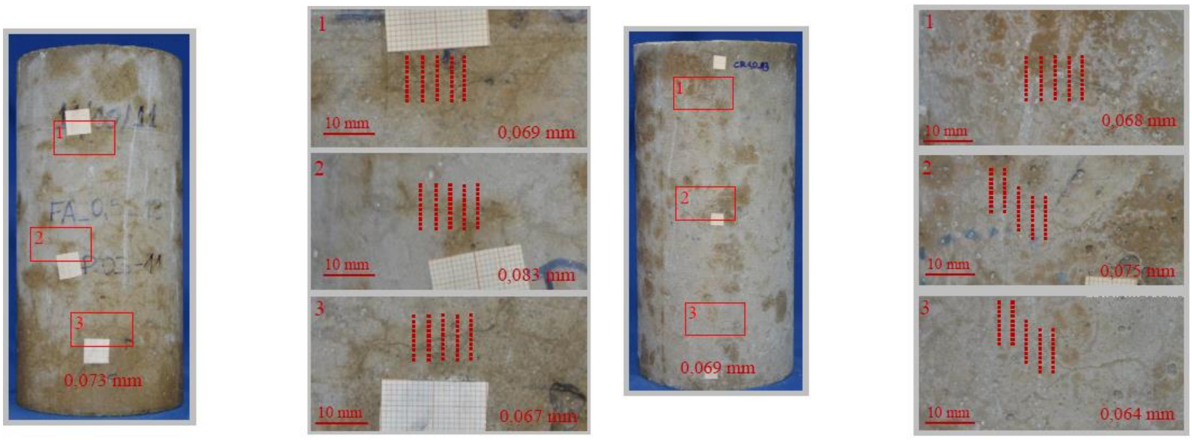

(a) (b)

Figure 4.11: Typical cracking at 365 days: (a) FC_0.5_13; (b). FC_1.0_13

In Table 4.3 we show the crack openings at 365 days for the several concretes.

Table 4.3: Crack opening (mm) at 365 days

	Top	Center	Bottom	Average
RC	0.107	0.163	0.208	0.159
FC_0.5_60	0.071	0.072	0.069	0.071
FC_1.0_60	0.092	0.108	0.111	0.104
FC_0.5_13	0.062	0.080	0.074	0.072
FC_1.0_13	0.065	0.060	0.069	0.064

It was observed that for the reference concrete there was an intense micro cracking in the sample, showing well-defined crack opening. In general, map cracking was observed, however, the orientation of the cracking occurred predominantly diagonally and horizontally. In the case of concretes containing fibers, the micro-cracking of the specimens was also observed in all concretes, with well-defined crack opening. The crack opening measured in all fiber reinforced concretes was much lower than that crack openings of the reference concrete. The results indicated also that cracks open less in concrete with 13 mm fibers.

4.4 Dispersion of fibers - X-Ray Computed Microtomography (XCT)

X-ray computerized microtomography (XCT) was performed at the end of the test on the five reactive concrete mixtures developed for the preventive part of the present work. We used a Skyscan Model 1173 Bruker microtomograph. The samples submitted to microtomography corresponded to the central part of the cylindrical samples used in the expansion tests. From these samples, a prism was removed from the central region of the cylinder and left in the dimensions of 50 mm x 50 mm x 75 mm for the acquisition of images (largest dimension allowed by the equipment), as shown in Figure 4.12.

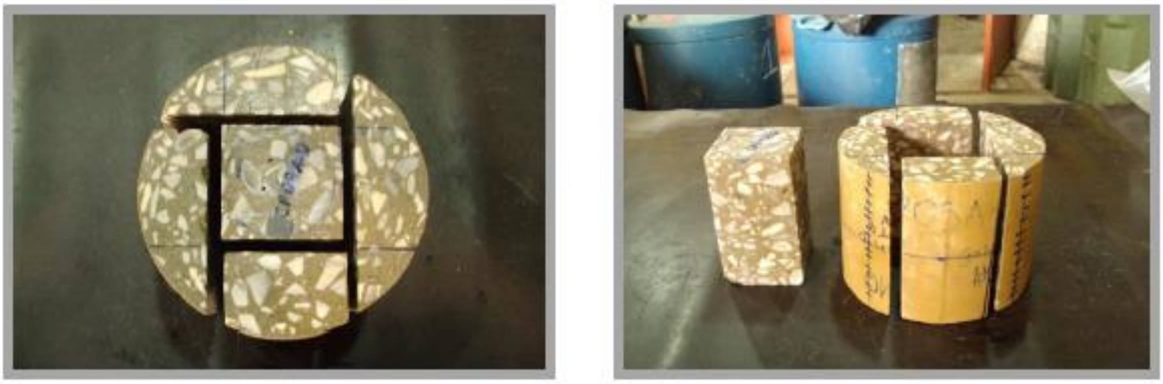

(a) (b)

Figure 4.12: (a) Cross section of the specimen; (b) 50 mm x 50 mm x 75 mm prism used for microtomography.

Figure 4.13 presents the images obtained by XCT, in which it is possible to observe the disposition of the steel fibers inside the fiber reinforced concrete specimens.

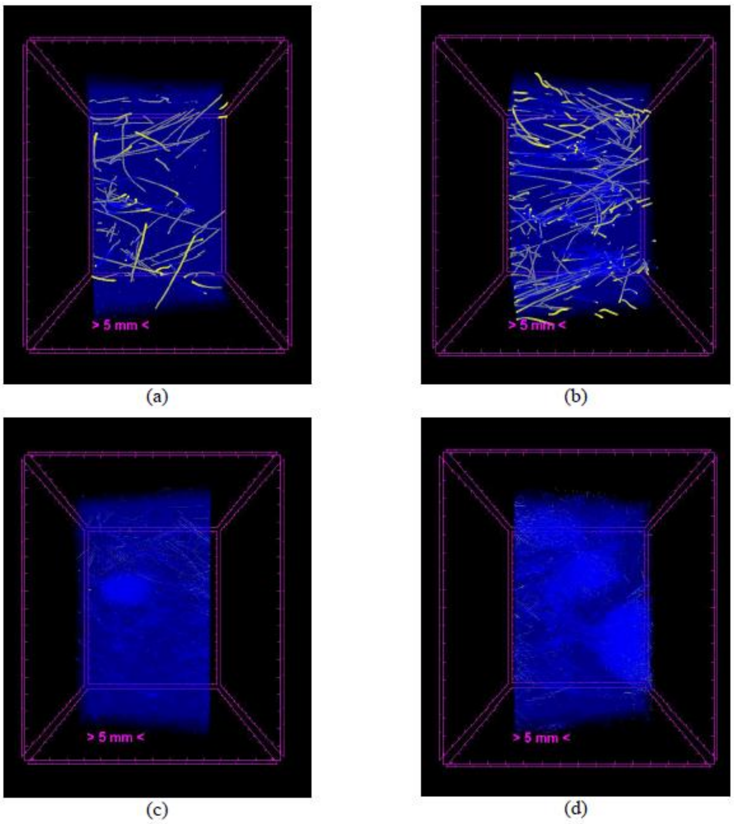

Figure 4.13: Fiber arrangement in fiber reinforced concretes: (a) FC_0.5_60; (b) FC_1,0_60; (c) FC_0.5_13; (d) FC_1,0_13

In regard to the 60 mm fibers, it is observed that FC_0.5_60 showed a random distribution of the fibers. For FC_1,0_60, greater stratification of the fibers was observed. This behavior is due to the vibration of the concrete during the pouring, since this mixture does not have a high fluidity. Therefore, it was necessary to perform the vibration of the concrete for a better accommodation in the mold. In the case of concretes reinforced with 13 mm fibers, the distribution occurred at random. However, there was the formation of skeins, especially in the mixture with the volumetric content of 1.0%.

5. CONCLUDING REMARKS

All fiber reinforced concretes developed for the present work were efficient in controlling the expansion caused by AAR. However, for long fibers, there was a saturation in the volume of fibers used, since the contents of 0.5% and 1.0 % presented the same magnitude of expansion for the two contents of fibers. For short fibers, it was seen that the concrete with the highest content of fibers showed a greater reduction in expansion. The efficiency of the fibers in the control of AAR was only observed after 90 days of immersion in the NaOH solution. This fact can be explained because the mechanical action of the fibers occurs as long as there is cracking or micro-cracking. However, at the end of the test, fibrous concretes can reduce the expansion of the reference concrete by half. This reduction can be very useful in constructions such as hydroelectric power plants when the use of potentially reactive aggregates cannot be avoided since the long-distance transport of the aggregates can make the construction unfeasible.

6. ACKNOWLEDGEMENTS

This study was financed in part by the Coordenação de Aperfeiçoamento de Pessoal de Nível Superior - Brasil (CAPES) - Finance Code 001. The authors also acknowledge the financial support of the Brazilian Scientific Agencies CNPq and FAPERJ, as well as National Electrical Energy Agency ANEEL and the Brazilian power company FURNAS.

7. REFERENCES

[1] Sims, I., Pole, A. B. eds (2017) Alkali-Aggregate Reaction in Concrete: A World Review, CRC Press.

[2] Turanli, L.; Shomglin, K.; Ostertag, C. P.; and Monteiro, P. J. M. (2001) Reduction in alkali-silica expansion due to steel microfibers, Cement and Concrete Research, V. 31, pp 827-835.

[3] Garci Juenger, M. C., and Ostertag, C. P. (2002) Effect of selective positioning of steel microfibers on alkali-silica reaction, Concrete Science and Engineering, V. 4, pp 91-97.

[4] Ostertag, C. P.; Yi, C., Monteiro, P. J. M. (2007) Effect of confinement on properties and characteristics of alkali-silica reaction gel, ACI Materials Journal, V. 104, No. 3, pp 276-282.

[5] Haddad, R. H., and Smadi, M. M. (2004) Role of fibers in controlling unrestrained expansion and arresting cracking in Portland cement concrete undergoing alkali-silica reaction, Cement and Concrete Research, V. 34, pp 103-108.

[6] Park, S. B., and Lee, B. C. (2004) Studies on Expansion Properties in Mortar Containing Waste Glass and Fibres, Cement and Concrete Research, V. 34, pp 1145-1152.

[7] Carvalho, M. R. P., Fairbairn, E. M. R, Todelo Filho, R. D., Cordeiro, G. C., Hasparyk, N. P., (2010) Influence of steel fibers on the development of alkali-aggregate reaction, Cement and Concrete Research, V. 40, pp 598–604.

[8] Yazici, H. (2012) The effect of steel micro-fibers on ASR expansion and mechanical properties of mortars, Construction and Building Materials, v. 30, pp 607-615.

[9] Beglarigale, A. and Yazici, H. (2013) The effect of alkali-silica reaction on steel fiber-matrix bond characteristics of cement based mortars, Construction and Building Materials, v. 47, pp 845-860.

[10] RILEM B - TC 106-3 (2000) Detection of potential alkali-reactivity of aggregates - Method for aggregate combinations using concrete prisms.

[11] ASTM C-1293 (2005) Standard Test Method for determination of length change of concrete due alkali-silica reaction.

[12] NBR 15577-6 (2008) Aggregates - Alkali-aggregate reactivity - Part 6: Determination of expansion on concrete prisms.

[13] JSCE-SF4 (1984) Method of tests for flexural strength and flexural toughness of steel fiber reinforced concrete", Concrete library of JSCE, Part III-2 Method of tests for steel fiber reinforced concrete, n. 3, pp 58-61.

[14] Águas, MFF, et al (2016) Influence of sugarcane bagasse ash in the expansions of mortars affected by alkali-silica reaction. Proceedings of the 15th ICAAR, São Paulo, Brazil.

[15] Larive, C (1997) Apport combinés de l´expérimentation et de la modélisation à la comprehension de l´alcali-reaction et ses effets mécaniques. Thesis (PhD), École Nationale des Ponts et Chaussées, Paris, France.